ELSEVIER

Journal of Volcanology and Geothermal Research 94 (1999) 251–265

Journal of volcanology and geothermal research

www.elsevier.com/locate/jvolgeores

Ground deformation monitoring of a potential landslide at La Palma, Canary Islands

J.L. Moss *, W.J. McGuire, D. Page

Geography and Environmental Management Research Unit, Cheltenham and Gloucester College of Higher Education, Francis Close Hall, Swindon Road, Cheltenham, GL50 4AZ, UK

Benfield Grieg Hazard Research Centre, Department of Geological Sciences, University College London, Gower Street, London, WC1E 6BT, UK

Department of Geomatics, Newcastle University, Newcastle, Ontario, Canada NE4 7SA

Received 10 May 1999

Abstract

The southern part of the island of La Palma comprises a north–south-oriented volcano known as the Cumbre Vieja. The steep gradient and high aspect ratio of the volcano, coupled with the prospect of future episodes of magma intrusion, highlight the potential for large-scale lateral collapse of the volcano, as recorded earlier in the history of La Palma and elsewhere in the Canary Islands. Historic eruptions of the Cumbre Vieja have occurred high up on the western flank of the volcano and along a single rift zone along the crest of the volcano. The geometry of the recent activity and faulting which occurred during an eruption in 1949 indicates that a discontinuity may be present beneath the western flank of the volcano, along which a future collapse may occur. To identify any displacement of the western flank overlying the discontinuity, a ground deformation network has recently been established on the volcano. The initial network spanned the fault system that developed on the upper flanks of the Cumbre Vieja during the 1949 eruption. This small network was measured in 1994, 1996 and 1997 using infrared Electronic Distance Measurement. In 1997, the network was enlarged and re-occupied, using the Global Positioning System, to incorporate the west flank and the southern part of the island. Although the results show that apparent displacements recorded during this period are within the error-margins of the techniques employed, the apparent movement vectors do suggest a coherent westward displacement of stations to the west of the 1949 fault system. Additional occupations of the network over the next few years will, however, be required to determine the reality or otherwise of this apparent coherent movement, and thus to decide whether or not the western flank of the Cumbre Vieja is currently sliding seaward. If not, it can be inferred that the volcano is stable during inter-eruptive periods.

Keywords: La Palma; ground deformation monitoring; flank collapse; Global Positioning System

1. Large-scale volcano instability in the Canary Islands

The Canary Islands have formed above a hotspot on the Atlantic oceanic plate close to the African

* Corresponding author. Tel.: +44-1242-543389; fax: +44-1242-532997; E-mail: jmoss@chelt.ac.uk

0377-0273/99/$ - see front matter
PII: S0377-0273(99)00106-7

continental margin (Carracedo et al., 1997a), see Fig. 1. The hotspot is presently located in the vicinity of the youngest and westernmost islands, La Palma and El Hierro. The volcanoes evolve in a pattern similar to that recognised in Hawaii (Walker, 1990), which is characterised by rapid shield growth followed by a period of inactivity with subsequent strong erosion, succeeded by a further post-erosional stage of activity that is labelled the *gap stage* (Carracedo et al., 1998). There is evidence of persistent flank collapse during the shield stage from Tenerife, El Hierro, La Palma and Gran Canaria, in the form of huge topographic scars in the island and off-shore deposits of blocky volcanic debris (Holcomb and Searle, 1991; Carracedo, 1994; Masson, 1996; Funck and Schmincke, 1998). The same phenomenon is believed to occur in other island and coastal volcanoes such as Hawaii, Réunion island (Duffield et al., 1982), Fogo (Day et al., 1999-this volume) and Mt. Etna (McGuire, 1996).

La Palma (28°N 17°W) is in the northwest of the archipelago and is the second youngest of the seven islands. It measures 45 km (N–S) by 30 km (E–W). The island is comprised of three sub-aerial volcanoes: Taburiente–Cumbre Nueva, Bejenado and the currently active Cumbre Vieja volcano (Carracedo et al., in press). Taburiente–Cumbre Nueva forms the northern part of the island and it developed on an uplifted and tilted seamount series. The volcano is comprised of lava flows and coherent dyke swarms with a single predominant north–south rift-zone called the Cumbre Nueva. This rift-zone formed a steep topographic ridge which collapsed to the west soon after 566 ± 5 ka (Guillou et al., 1998). The small Bejenado volcano grew in the collapse scar and did not undergo lateral collapse.

1.1. Geological evolution of the Cumbre Vieja, La Palma

The Cumbre Vieja volcano began to develop on top of the remains of the collapsed Cumbre Nueva ridge about 125 ka BP (Guillou et al., 1998). Intense eruptive activity continued until 80 ka BP and was followed by a quieter strongly erosional period which ended in 20 ka BP. The Cumbre Vieja has grown through successive eruptions to form a steep sided, high aspect, topographic ridge with slopes of 16°–20°; it has a current sub-aerial area of 220 km^2 and an estimated volume of 125 km^3 (Carracedo et al., 1997b), see Fig. 2. There is evidence from volcanic cone distribution and orientation patterns for an initial triple-rift stage in the development of the volcano with rift-zones located roughly 120° apart ori-

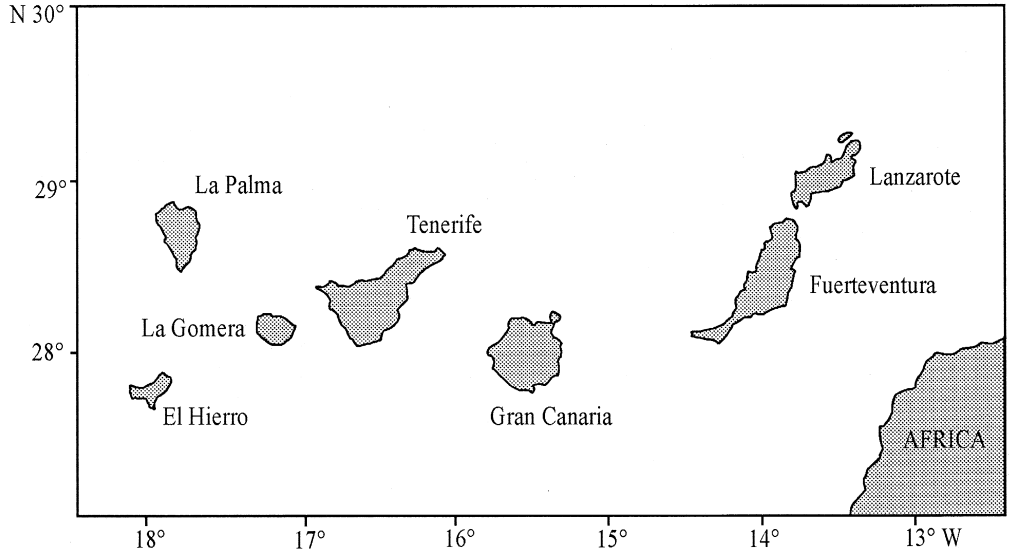

Fig. 1. Location map of the Canary Islands in the Atlantic Ocean, 200 km west of Morocco, Africa.

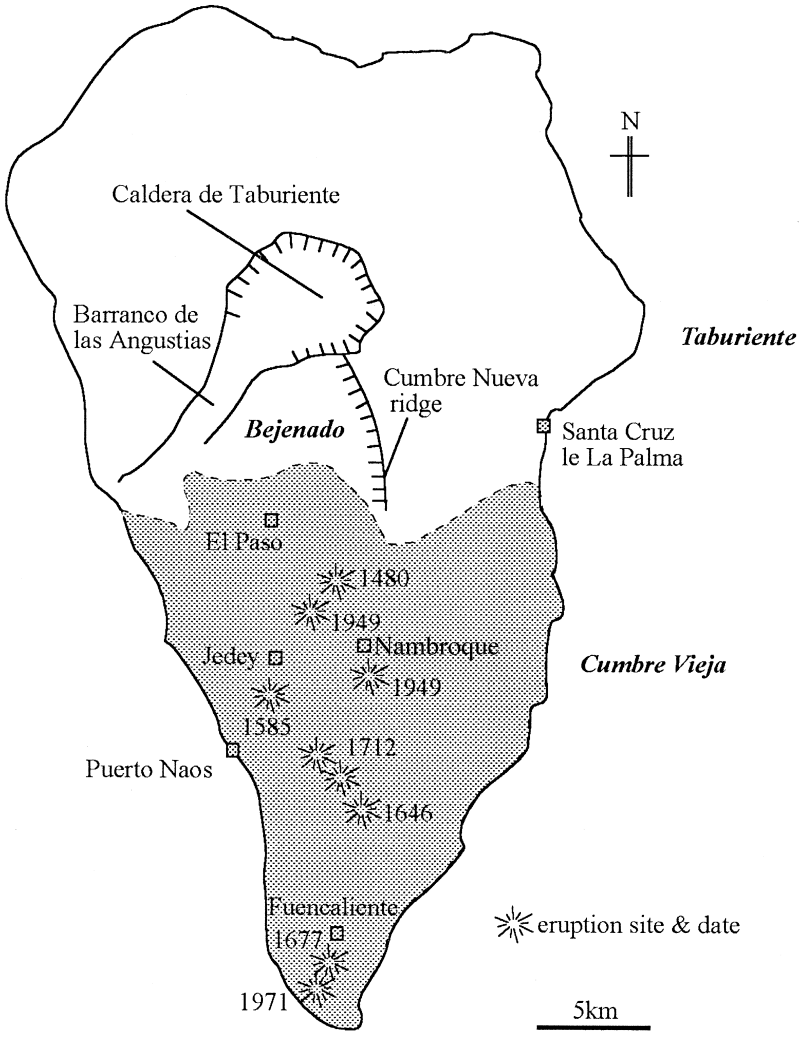

Fig. 2. A simplified sketch map of La Palma indicating the volcanic edifices and the historic eruption sites.

ented northeast, northwest and south (Carracedo, 1994; Day et al., 1999-this volume). The rift-junction centre of this early edifice, was located at Nambroque on the highest part of the summit ridge (Fig. 2). From 20 to 7 ka BP activity was sustained along all three rifts until a reorganisation of the plumbing system occurred, with subsequent dominance and northward propagation of the southern rift. Eruptions along the NW and NE rifts stopped.

1.2. 1949 Eruption of the Cumbre Vieja

During the eruption of 1949, and for the first time in some tens of thousands of years, normal fault ruptures developed along the crest of the volcano. For reasons discussed elsewhere (Day et al., 1999-this volume), these faults are unlikely to be associated with a near-surface intrusion. Instead, they are thought to be the first surface ruptures produced by a developing detachment fault or zone under the western flank of the edifice (Day et al., 1999-this volume). The asymmetry in the structure of the volcano implies that this may reflect the substrate on which it grew. After the collapse of the Cumbre Nueva, sediments would have been deposited onto the western flank, this weak layer coupled with the steep collapse scar, would have formed a weaker boundary between

the sediments and the new Cumbre Vieja lavas, than on the eastern flank boundary on the other side of the ridge. This weak boundary is likely to have become the inferred detachment structure.

In 1971, an eruption occurred near the southern tip of the island, where the ridge is lower and shallower. This eruption did not produce a similar array of faults to the 1949 eruption near the highest point of the ridge, suggesting either that the region of instability does not extend to the south end of the island or that magma did not rise high enough in the volcano to trigger flank movement, in contrast to the situation in 1949. The eruption did cause the development of eruptive fissures and associated seismicity.

Carracedo et al. (this volume) speculate that a future eruption close to the ridge crest may trigger a lateral collapse of a substantial part of the western flank of the volcano. This may either abort, as in 1949, or continue into the sea, posing a significant tsunami threat within the Atlantic Basin. The likely trigger for collapse initiation is dyke emplacement parallel to the length of the ridge, with either mechanical push, thermal effects on pore waters, or a combination of the two providing the impetus for failure (Elsworth and Voight, 1995, 1996).

The sub-aerial part of the potentially unstable sector of the Cumbre Vieja is around 20 km long and up to 8 km wide. The northern boundary of the potential slip zone is inferred (Day et al., 1999-this volume) to be north of the San Juan fissures, where in 1949 en echelon fissures opened perpendicular to the N–S alignment of the rift. The southern boundary is likely to be in the vicinity of the southern tip of the island but its precise position is presently unknown: the distribution of geodetic stations in this area (see below) is in part designed to help constrain the position of this boundary. Future dyke intrusion could cause westward displacement of this unstable sector culminating in failure of the western flank of the ridge.

2. Ground deformation monitoring

The island of La Palma does not have, at the time of writing, any real-time continuous monitoring. In recent years, a single seismometer has been used to record background seismicity, however, due to persistent vandalism and technical problems the data have not been continuous. From the limited data set collected and the perceptions of the islanders (J.C. Carracedo, pers. commun.), it appears that there have been no significant seismic events since the last eruption in 1971. The establishment of the ground deformation monitoring programme facilitates analysis of the current stability of the ridge. The creation and repeated re-measurement of the baseline network described here will with time provide increasingly tight constraints on the level of inter-eruptive ground deformation occurring on the island, such that in the event of a future intrusion of magma or the dislocation of the western flank the deviation from the background levels could be accurately assessed. If creep is detected around the 1949 fault between eruptive events then future failure may not necessarily be linked to magmatic activity. This would have major implications for the level of hazard in the island (see Section 5). The deformation of the whole island can also record the current rates of either uplift or subsidence. Klügel (pers. commun., 1997) and McGuire (pers. commun., 1997) speculated that broad uplift over the whole island could occur prior to an eruption as is commonly the case on other volcanoes.

2.1. Instrumentation: techniques and errors

Changes in the ground surface are monitored through the periodic measurement of a network of survey stations. The survey stations of the network may be positioned by either measuring vector and distance measurements between markers using Electronic Distance Measurement (EDM) or through the measurement of their three dimensional position relative to a fixed point using the Global Positioning System (GPS). A combination of EDM and GPS was used at various times in the installation and occupation of the full network of survey stations, as described below. The accuracy of the data are determined through a combination of different factors including, the physical set-up and measurement (listed in Table 1), technique precision and theoretical errors determined by the geometry of the network and the covariance matrix from the least squares adjustment of the data. The data are represented in

Table 1
The range of errors experienced the Sokkia Set3c Total Station used in this study (after Uren and Price, 1994)

Sokkia Set3c Total Station	Type	Estimated error
Distance measurement error	Random	3 mm + 3 ppm
Vertical angle measurement	Random	±3″
Temperature 1°C variation	Random	1 ppm
Pressure 3 mm Hg variation	Random	1 ppm
Setting up error	Random	1–2 mm
Internal instrument errors	Systematic	unknown
Prism pointing	Random	±0.5–1 mm

this study as vectors with theoretical error ellipse values. It must be stressed that these error ellipses reflect only the internal reliability of the data and the network design and do not reflect external error sources such as user error or environmental factors (Table 1). Although the error ellipses are important as a lower limit on the true errors, the estimated error for the application of each technique in the field needs to be borne in mind during the interpretation of the data.

2.1.1. EDM

A Total Station combining an EDM and theodolite was used from 1994 to 1997 to establish and re-measure the first stations of the ground deformation network in La Palma. The Total Station and retroreflectors are set up using tribrachs and tripods over the permanent markers to achieve a high accuracy. The types of errors that may result during the survey station occupation are listed in Table 1. The predicted set-up accuracy is to within 1–2 mm depending on the marker installed for the survey station and the weather conditions during measurement. The most common marker used is a steel 10×100 mm survey nail hammered into a rock or stable feature. In loose material, the markers are sections of steel reinforcing rods, up to 100 cm long, hammered into the ground. A few existing survey pillars are incorporated into this network; however, it was found that the errors in instrument location above these survey pillars are twice as bad as for a survey nail due to the absence of permanent baseplates on the top of the pillars. Repeated measurements are undertaken during each station occupation to reduce the magnitude of the errors caused by tropospheric conditions and user mistakes. The most important of the latter occur along lines over 2 km, which commonly experience *pointing errors*. These occur when the user fails to aim the instrument exactly on the positioning-target which is placed over the reflectors in order to maximise the potential accuracy. On completion of a station occupation, the data from these repeated measurements are then averaged to give a final measured value. These measured values are then adjusted as follows:

(1) The prism offsets are accounted for and internal instrument errors are removed.

(2) Temperature and pressure corrections, necessary because of changes along the measurement vector, are made. The necessary pressure and temperature corrections are determined using averaged readings taken at the ends of each line.

In order to identify and distinguish instrumental, set-up and other errors from real movements of the survey stations (whether due to volcanic unrest or local slope instability), the measurements were systematically analysed. The first step was to examine the data for anomalous measurements. In most cases, these are spurious results that usually result from user oversight or extreme weather conditions, and can be identified from inconsistencies between lines sharing one common station (hence, one of the reasons for the importance of generating ''well-braced'' measurement polygons in which the position of any one station is measured relative to a number of other stations). The data from later surveys were compared with the data collected in earlier surveys to identify any anomalously large changes in line lengths.

The checked changes in line length and vertical difference are examined through the following two approaches:

(1) The changes between one survey and the next data are plotted against the baseline length to check for errors which are attributable to the length of the baseline or the meteorological conditions at the time of the measurement. The expected level of error can in general be represented as a linear function of line length L plotted on the graph: changes which plot above this line are those which are most likely to be significant. In the diagrams plotted in this paper, the error limit $(10\ \text{mm} + 0.000003L)$ is plotted as an illustration of the likely level of error: this is discussed further in Section 4.

(2) The strain rates for each line are analysed, these are dependent upon setting-up errors and measurement errors.

The EDM distance measurements and vertical angles were then converted into grid coordinates using a programme called LSXY (Crook, 1984). The algorithm fixed the azimuth of one vector and the height of one survey station. A least squares estimate was then applied to fit the measured vectors to a second set of vectors obtained from an approximate set of grid coordinates. Error ellipses were obtained for each coordinate. If the network then appears to have rotated around a single station, a spreadsheet-formula is used (Pullen, unpublished) to un-rotate the data as such a rotation is physically improbable and is more likely to be an artefact. As the coordinates are calculated using both the distances and the vertical angles measured between the survey stations, the accuracy of the final coordinate is reduced by the errors of both measurements and therefore has a potentially greater error, as represented by the error ellipses.

2.1.2. GPS

The GPS is a satellite surveying system designed to locate unknown positions on the surface of the Earth. A full description of the use and application of GPS to surveying and to deformation studies may be found in Hofmann-Wellenhof et al. (1997). The La Palma GPS network has been measured using differential rapid–static and differential static GPS. Differential GPS techniques use two or more GPS receivers simultaneously. One receiver (*reference receiver*) is left at a location whose position is considered fixed for the duration of the measurement session and programmed to repeatedly determine its position. Apparent variations in its position are due to signal degredation errors (including Selective Availability or the encoding of parts of the satellite signal) which can be calculated for every location determination this receiver makes. The errors determined by the reference receiver are subsequently removed from the corresponding satellite measurements made by the other receivers at their unknown locations. The assumption that similar atmospheric effects occur along the signal paths from the satellites to both stations limits the maximum distance between the receiver and the rover to 10 km. However, once a survey station has been occupied by the second receiver (at least twice), then it can be used as a new reference location, allowing the progressive occupation of networks more than 10 km across. The use of rapid static GPS differs from static GPS in that the occupation times for the *roving receivers* is very short (5–20 min for baselines less than 10 km) as opposed to 60–120 min for static GPS: this allows a large number of survey stations to be measured in a short time.

Precise geodetic surveying is accurate to approximately 10 mm + 1 ppm for rapid–static GPS under optimal conditions. Owing to the geometry of the satellite orbits which define the framework to which the locations of the stations are measured, the errors are significantly greater in the vertical plane than in the horizontal plane (see Section 4.2). The accuracy of GPS in the field is degraded by set-up errors and the environmental influences such as multipath or severe tropospheric variations. The application of the rapid static technique can further degrade the accuracy to approximately 10–15 mm $\pm$ 3 ppm: however, it has the advantage of being able to measure large numbers of survey stations over a very short time.

The data are downloaded from the receiver to a laptop computer, the receiver set-up information is checked and the data are examined for breaks in signal reception or a lack of data from common satellites between the reference and the rover receivers. A detailed explanation of the GPS data processing is beyond the scope of this paper: the methods are described further by Blewitt (1997), Hofmann-Wellenhof et al. (1997) and Moss (1999). Briefly, for each session the data are processed using a combination of code and phase processing to produce an L1 code fixed double difference solution and the whole network is combined in a network (least squares) adjustment.

3. Measuring the ridge and flank networks

The network was established in two stages; firstly, an initial small network covering the faults at the summit of the Cumbre Vieja and secondly the expansion to from a broad-scale network encompassing the southern part of the island (south of Caldera de

Taburiente). This two-stage approach reflects the change in technique from EDM to GPS in 1997, which allowed the enlargement of the network to cover the southern part of the island. As discussed above, the deformation analysis aimed to determine if the 1949 fault was stable or undergoing aseismic fault creep. Further objectives, if movement were present, were to define the spatial distribution of deformation around the 1949 faults (in the case of the summit network) or the whole of the unstable sector (in the case of the large network).

The anticipated displacements associated with eruptions and other events are the following:

(1) From measurements undertaken in Hawaii and on Etna, it can be confidently stated that the expected displacement values for a forceful shallow dyke intrusion are in the magnitude of 500 mm and above (Swanson et al., 1976; Dzurisin et al., 1984; HVO monthly reports; Pollard et al., 1993; Nunnari and Puglisi, 1994; McGuire, 1996).

(2) The values for deeper magmatic or tectonic influences are 25 mm and above (Murray and Pullen, 1984; Yang et al., 1992).

(3) Displacements associated with another episode of faulting comparable to that which occurred in 1949 (Day et al., 1999-this volume) are of the order of a few metres.

3.1. The installation of the ridge network

The preliminary ground deformation network (''ridge network'') was established over the 1949 fault system mapped by Day et al. (1999-this volume) to assess if a seismic creep was occurring during the current inter-eruptive period. The 11 survey stations of the ridge network were installed and occupied in 1994 using infrared EDM and a theodolite. The spatial distribution of the survey stations was controlled by (I) the surface traces of the 1949 fault system and (II) the limitations of the EDM technique. This latter consideration is influential since the majority of the survey stations are required to be inter-visible in order to maintain a well braced measurement polygon and thus both redundancy and cross-checks on the measurements (Fig. 3). Most of the survey stations were therefore installed on elevated cones and two survey stations were located off the ridge to the west, where gaps in the tree cover allowed line-of-sight to be maintained. Unfortunately, these off-ridge survey stations (pr11 and pt10) were at the limit of the EDM horizontal (2.5 km) and vertical range (500 m) and good coordinate fixes were not obtained due to the poor repeatability of these measurements. The coordinates for the whole network were therefore calculated relative to a survey station on top of the ridge but at least 1000 m from the fault. Although the best procedure practicable, this was not ideal, as it should not be assumed that any of the ridge stations are stable: the overall deformation field may extend well beyond the ridge network and so the network will only measure a fraction of the overall deformation.

The network was measured during its installation in 1994 and was then re-occupied using the same technique in March 1996. This data can be taken as the *baseline data-set* as no eruptive or tectonic activity was recorded during this time. The EDM data were transformed into grid coordinates using the method outlined earlier: however, these results had rather large error ellipses due to the poor repeatability of vertical angle measurements. The vector velocity changes examined later are relative to the station AV06, which is held fixed.

The use of EDM proved unsatisfactory for a number of reasons:

(1) Deformation data are only relative to one station located along the apex of the rift, it should not be assumed that at any one time all the survey stations would be stable. The line length and vertical angle changes between survey station are satisfactory and represent the real deformation between individual survey stations, however, the vector displacements relative to one point may be erroneous and should be interpreted with caution.

(2) The ridge network could not be extended to cover the western flank using the EDM technique, as there are no suitable locations for stable survey stations immediately beyond the network and the maximum measurable distance of the technique is limited to about 2 and 2.5 km (where two sets of triple prism reflectors are used).

(3) The weather proved problematic for the EDM technique: although the average temperature is around 20°C and both pressure and temperature gradients are stable, low clouds frequently cover the ridge and block the EDM signals.

Due to these problems the expansion of the flank network was undertaken using GPS.

3.2. Installation of the flank network

The flank network encompasses the ridge network and the whole western flank of the Cumbre Vieja ridge, providing tight clusters of survey stations in the regions where the northern and southern boundaries of the unstable zone may be located and at the apex where the 1949 fault is situated (Fig. 4). The design of the network was completed using the geological map (Carracedo et al., 1997c) and in consultation with Simon Day. The network com-

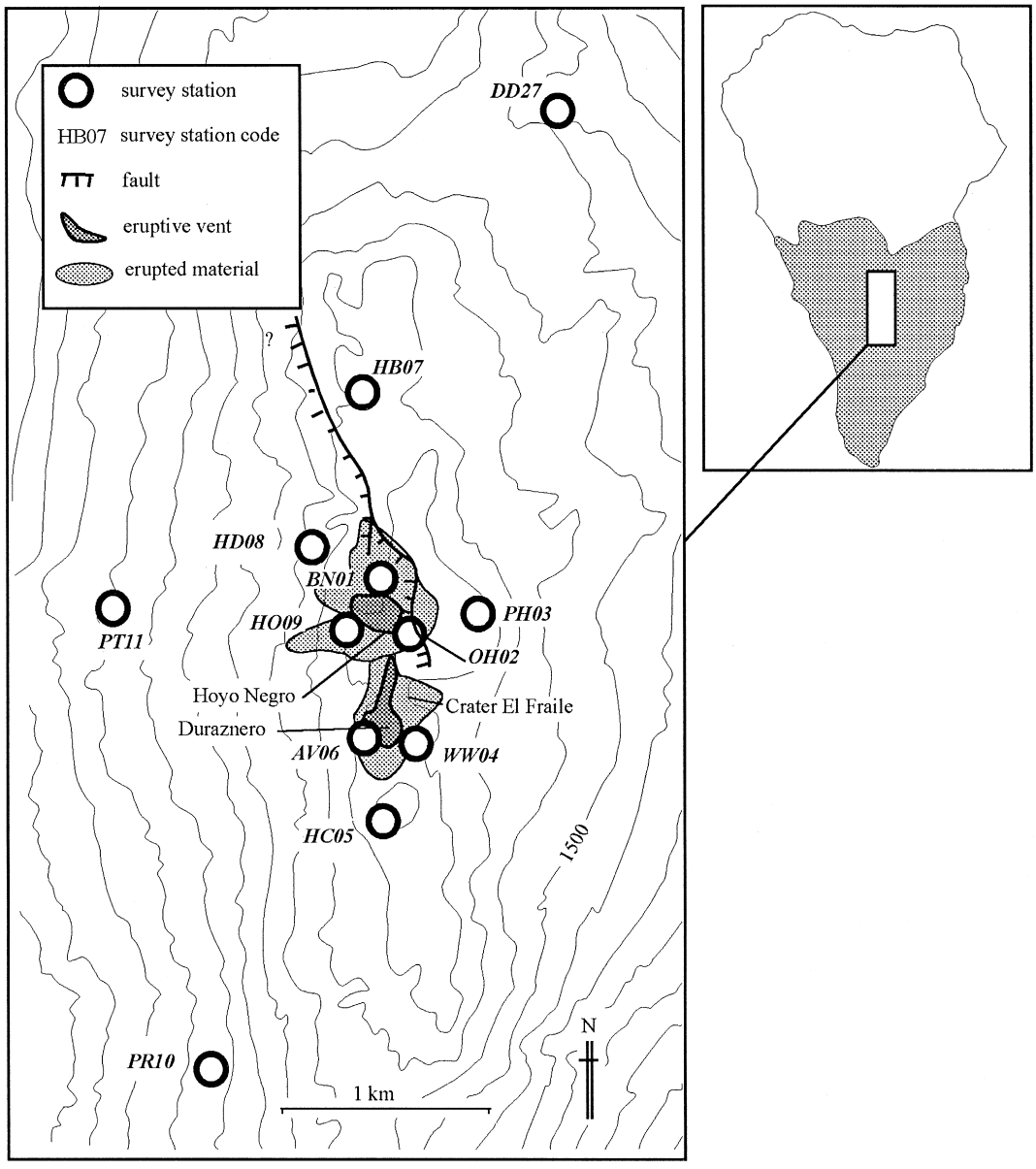

Fig. 3. A sketch map of the ridge network showing the positions of the survey stations relative to the 1949 eruption vents and fault system.

prises 26 survey stations which are a combination of small nail and rods markers and survey pillars.

4. Deformation results 1994–1997

4.1. The ridge network

The ridge network was occupied in 1994, 1996 and 1997. In 1994, 20 lines of the 22 within the network were measured: the two lines (both over 1.9 km) that were not measured were blocked by persistent cloud. In 1996, 21 lines were measured, once again the missing measurement was unobtainable due to cloud. The two longest vectors in the network are over 2.5 km and were measured during the 1996 survey using a fully charged battery and two sets of reflectors in very clear conditions. In 1997, eight lines were measured using both EDM and GPS in order to compare simultaneous readings.

The results from the 1994 and 1996 EDM surveys indicate that the majority of baseline distance changes between the survey stations were of the order of 4 mm. A few line-length differences of 8–10 mm occurred along the long lines with large height differences and for lines measured to pillar-based survey stations (with no fixed baseplates). The estimated error for the EDM method is 5 mm $\pm$ 3 ppm of line length (sigma) for a single survey and twice this for comparisons between two surveys. Table 2 shows the differences measured between common lines using the total station from October 1994 to March 1997 using a combination of EDM and GPS.

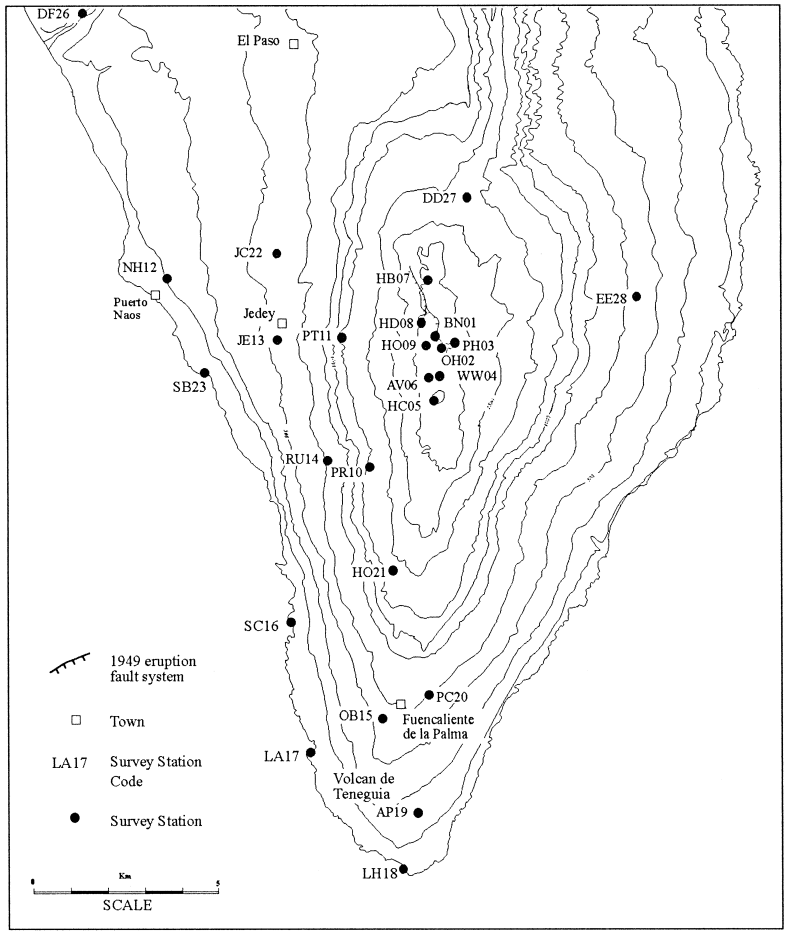

Fig. 4. A location map of the whole network showing the survey stations and the 1949 fault system.

Table 2
Changes in line length and vertical distance between line lengths measured in 1994, 1996 and 1997 on the ridge network using the EDM technique

Baseline between survey stations		1994–1996 (m) EDM error margins (5 mm ± 5 ppm)		1996–1997 (m) EDM and GPS error margins (10 mm ± 3 ppm)	
		Vertical distance	Line length	Vertical distance	Line length
2	3	0.022	0.008	−0.007	−0.005
5	3	0.016	0.006	−0.005	−0.003
9	1	0.005	−0.002	−0.002	0.0004
4	3	−0.017	0.006	0.012	0.004
1	3	0.001	−0.002	0.012	0.009
9	2	−0.001	0.002	0.012	−0.004
1	2	−0.003	0.003	0.018	−0.004
4	2	−0.003	0.001	0.035	0.0027

The measurement of vertical angles produces a larger differences in baseline length from one survey to another than the horizontal distance measurements.

To establish the real movement of any survey stations, the anticipated errors from either cloud-obscured readings or set-up inaccuracy were identified and eliminated from the results. This was achieved by assessing repeatability of measurements within the same survey and in consecutive surveys. Fig. 5 illustrates the repeatability of the measurements through the comparison of a single vectors between 1994 and 1997. The difference in the line length measured between one survey and the next is plotted against the baseline length. Error bars for each measurement represent one standard deviation. The estimated error is represented by the linear expression $\alpha + \beta L$, where $\alpha =$ (random + systematic) error, β = error in ppm of the baseline length and $L =$ baseline length. This represents the expected error for one survey (either from EDM or GPS) (α) and between two surveys (2α) (Nunnari and Puglisi, 1996; Savage and Prescott, 1997). The linear representations of sigma in Fig. 5 delimit the errors for the EDM (5 mm ± 5 ppm) and the GPS (10 mm ± 3 ppm) techniques. The values below this line are within the error margins of the techniques and can be considered insignificant. The vectors above this line indicate either very small movements or errors.

Five measurements plot above the error lines. Three of these are measurements to PH03, a pillar station which has no permanent baseplate thus degrading the set-up accuracy to approximately 5 mm and thus increasing the error expected in these measurements. One of the remaining two measurements

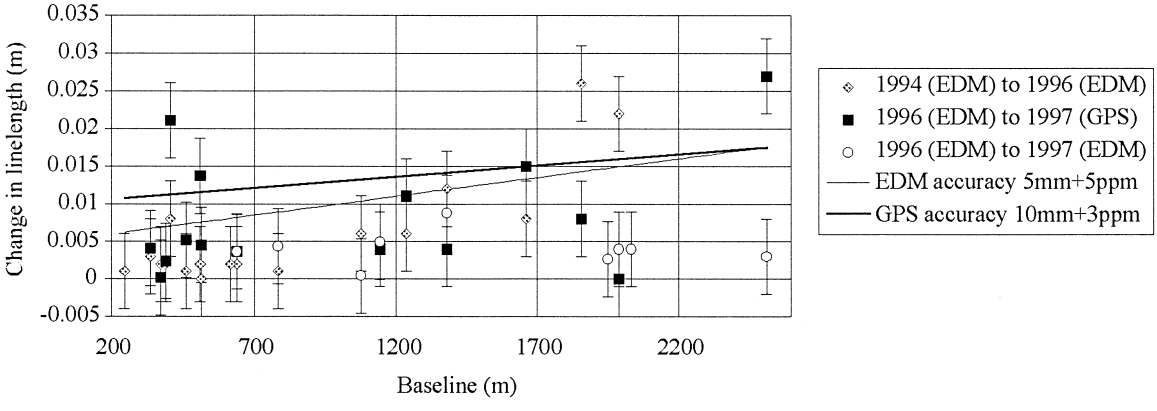

Fig. 5. Repeatability of the measurements illustrated by the comparison of vectors between 1994 and 1997.

spans a long distance with a large height difference, again increasing the possible error to above that represented by the error lines, but the final measurement cannot be explained. However, as this does not form part of a pattern, this reading is assumed to be spurious unless confirmed by future surveys.

Fig. 6 shows the vector movements of the ridge network between October 1994 and March 1996. The vectors are generated from the EDM data using a set of reference grid coordinates derived in 1997 using GPS location of the same stations. Error ellipses are generated with each set of coordinates, the error ellipses are generated from the calculation of the 1996 coordinate data-set and are therefore plotted with the vector displacements in Fig. 6.

The vectors represent apparent coordinate changes that are of a relatively small magnitude. If they are real they may be of various origins but a number of mechanisms can be excluded. Ground deformation associated with the shallow intrusion of magma measured on Kilauea (Hawaiian Volcano Observatory Monthly activity reports, 1966–1981; Delaney et al., 1990) and Etna (Murray, 1990; McGuire et al., 1997) is typically over 10 cm near the surface traces of a shallow intrusion. Deeper magmatic intrusions are frequently accompanied by deformation under 10 cm but would often be accompanied by seismic activity. The last eruption of the Cumbre Vieja was in 1971: there is no evidence of shallow magma storage since this time and a fresh intrusion of magma at depth would have most likely been accompanied by some felt seismic activity or other related activity such as fumarole formation and gas release.

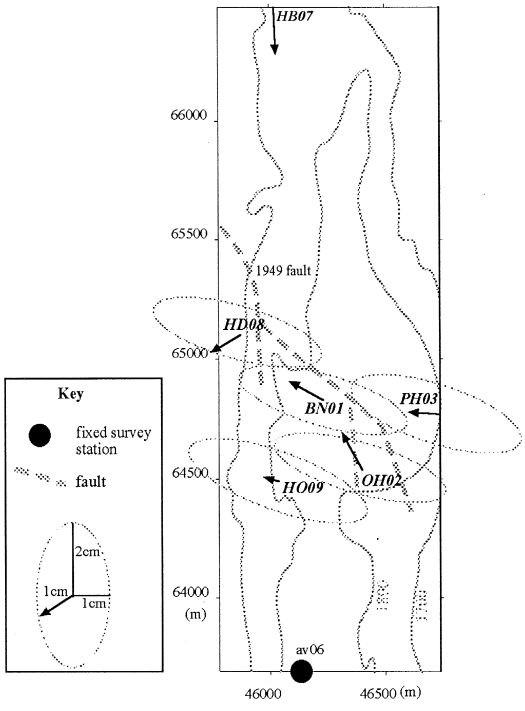

Fig. 6. Vector displacements between 1994 and 1996 including EDM error ellipses for 1996: there is no error ellipse available for station HB07.

The stations of HD08, BH01, PH03, HO09 and OH02 do, however, indicate a coherent pattern of westward displacement of the block on the western side of the summit fault traces. It would be imprudent at this stage to state that this pattern represents real movements, but the coherent changes may indicate a distinct block of stations within a westward sliding or creeping block. There appears to be no correlation between the aspect of the slope on which the survey station is situated and the direction or rate of movement, therefore eliminating a correlation between this displacement and localised slope creep or unstable survey station markers. The patterns of vector displacement are compared over time to distinguish coherent displacement of individual or groups of survey stations.

4.2. The flank network

The flank network was measured using the rapid static technique with two GPS receivers. A single station was occupied for 10 h each day for 3 days to obtain a single point position; this enabled the station to be used as a reference point. It must be stressed that this station is considered stable solely for the duration of the survey. To undertake the rapid static survey, one receiver was initially positioned at the reference point (NH12) and the other occupied adjacent survey stations. Since the flank network is more than 10 km across, it was necessary to move the reference station in subsequent measurement sessions as discussed above. Increasing the number of reference points away from the original single point (NH12) permitted the occupation of the whole network (except the survey station WW04 on the ridge network, which was not occupied due to strong winds rendering the site unsafe).

The majority of the survey stations were measured at least twice in order to obtain an exact coordinate location and to permit network adjustment. It was not possible to process the data in the field, so all the post-processing was completed after the field work. The post-processing was carried out using GYPSY and PRISM (ASHTECH) software. The absolute single point position of station NH12 was obtained using the UNIX based GYPSY software: this position was then kept fixed during an initial subsequent least squares network adjustment (but see below). The survey points of the network were processed from this fixed position using PRISM. During this initial run, it became apparent that at certain times the reference and rover receivers were not viewing enough common satellites to obtain the coordinate for the rover survey station. This was usually due to tree canopy above or adjacent to the rover survey station causing cycle-slips but in some cases, observations between the reference station and the rover failed without any identifiable reason. As most of the survey stations were occupied at least twice very few were totally lost, although coordinates were not obtained for stations PT11 and SC16.

Due to these observation failures, an additional single point position was obtained using GYPSY for OB15 to maintain the integrity of the network; this was held fixed and the southern survey stations processed from this position. The northern and southern parts of the network were network adjusted together using SNAP (PRISM, ASHTECH), holding the survey station JE13 fixed. The adjusted network comprised 39 vectors although the problems fixing the coordinates produced a few open-ended baselines.

The differences in the two techniques illustrated in Fig. 5 indicate that the data-set combining the two techniques produce a lower repeatability than when just EDM data-sets are compared. The average calculated horizontal-plane error ellipse for the GPS data is 0.723 cm (major) and 0.486 cm (minor), the average calculated vertical-plane error ellipse represents a lower accuracy at 1.58 cm (major) and 0.533 (minor). These error ellipses are with a 68% confidence interval. The poorer accuracy of vertical positioning is expected when undertaking rapid static GPS. The vector changes between 1996 and 1997 are compared in Fig. 7: they are within the 10–15 mm

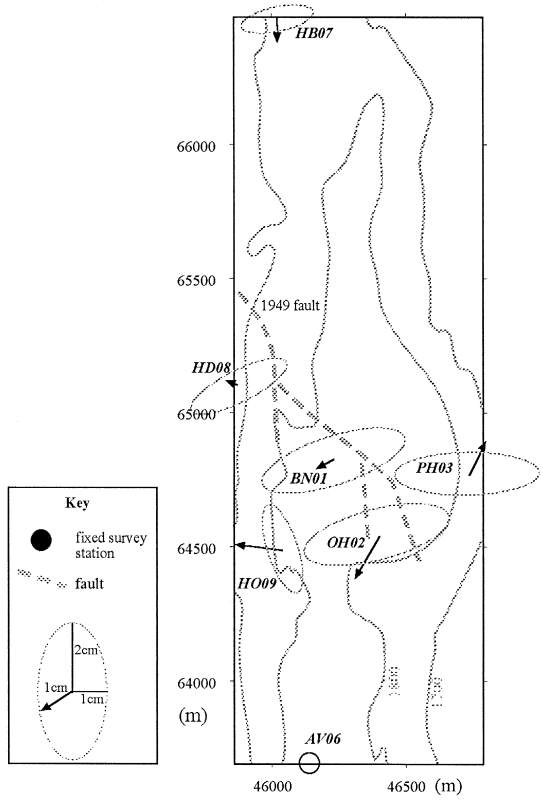

Fig. 7. Vector displacements between 1996 and 1997 including GPS error ellipses (1997).

error ellipse for the conversion of EDM data to coordinates. The vector changes do not indicate the same apparent coherent pattern observed between 1994 and 1996 (Section 3), but survey stations HD08, BN01, OH02 and HO09 do show a continued westward displacement. The coherent nature of the apparent movements does suggest that there may be a real, but very small, movement. The actual baseline length measurements of stations west of the fault also adhere to this pattern suggesting that the coherency is not an artefact of the transformation between EDM data and coordinates in 1996. In contrast, station PH03 (east of the 1949 fault system) shows inconsistent apparent displacement. Finally, station HB07 has been consistently displaced towards the south, but as this survey station is situated on a south-facing slope then the cause of this displacement is most likely slope creep. Fig. 8 illustrates the vector displacements of survey stations occupied in 1994 and

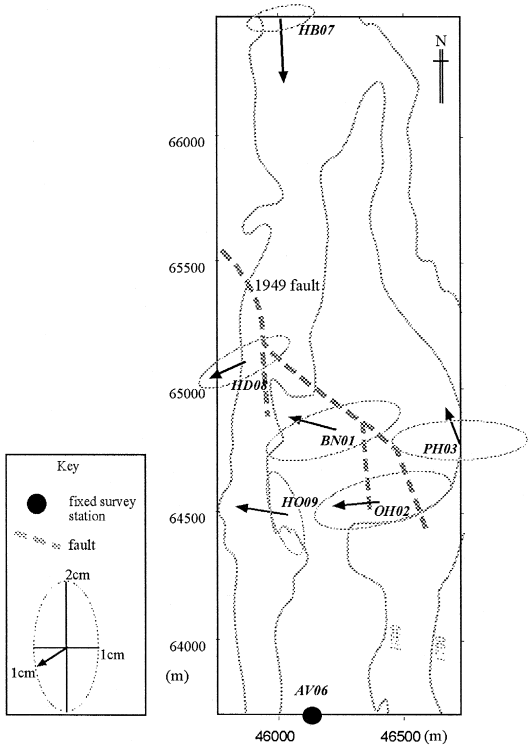

Fig. 8. Vector displacements between 1994 and 1997 including GPS error ellipses (1997).

1997. The 1997 (68% confidence interval) error ellipses are also included in this diagram.

Despite the small size of the apparent movements relative to the calculated error ellipses, the results of the surveys to date reveal an interesting pattern of potentially significant coherent data. The vector displacement had been consistently from the east to the west for the majority of the stations on the ridge which lie to the west of the surface trace of the 1949 fault system. The changes cannot be explained by the nature of the survey station marker (the differing aspects of the slopes on which the stations are installed argues against this). The results may indicate a very slow moving deformation that results from an inherent instability of the western flank. However, caution should be taken in extrapolating the data due to its small magnitude.

At this stage of the monitoring programme, care should be taken, for a number of reasons, in interpreting the data in terms of continued movement. Firstly, because the displacements involved are small, and secondly, because of potential additional inaccuracies arising through the transition from EDM to GPS. Clearly, several more re-occupations of the expanded GPS network are required to determine whether or not the detached mass is moving during the present inter-eruptive period, and if so, to constrain the nature of the movement. The next occupation of the network on La Palma will also be the first to provide displacements of the flank network: this may be a more sensitive indicator of instability since the survey stations span the whole of the sub-aerial part of the Cumbre Vieja volcano and thus will envelop most of the potentially unstable region.

5. Implications of ground deformation results on island instability

Although the EDM method proved suitable for monitoring the stability of the western flank of the Cumbre Vieja volcano, the need to expand the size of the network necessitated the transition to GPS, which has proved to be both more accurate and more flexible. Although acquired data do appear to indicate a coherent westerly movement of stations located on the upper flanks of the Cumbre Vieja, these are too small to be attributed to the shallow emplacement of magma. Furthermore, with the vector changes all within the error ellipses and accuracy of the data acquisition and processing techniques, interpretation of the coherency in terms of continued westward sliding of the western flank should also be treated with some caution. The small scale of the observed displacements, if real, might be attributable to creep along the 1949 faults, although the apparent westward movement of stations on both sides of the fault would appear to argue against this, at least since measurements began in 1994. Instead, a model of distributed displacement over the entire western flank might be a possibility. In either case, several further re-occupations of the enlarged GPS network will be required before any pattern of deformation can be determined with confidence.

In order to permit the recognition of island-wide deformation associated, for example, with the more widespread emplacement of magma at depth, it is planned that the network will be further expanded to include additional stations in the north of the island.

For hazard assessment purposes, establishing the presence or absence of continuing movement of the western flank of the Cumbre Vieja volcano is critical. Not only because, in the absence of additional monitoring, this is likely to provide the only indication of the emplacement of fresh magma beneath or within the edifice, but also because a future lateral collapse event is most likely to occur at such a time. The hazard implications of the entry into the sea of a mass of volcanic debris that may total two hundred cubic kilometres are particularly worrying, with resulting tsunami having the potential to impact on both sides of the Atlantic Basin. It must be stressed, however, that although it is likely that the western flank of the Cumbre Vieja volcano represents the youngest giant volcanic landslide on the planet, there is currently no evidence for imminent collapse.

Acknowledgements

The authors would like to thank Juan-Carlos Carracedo and Simon Day for their invaluable help and advice in the field and to Newcastle University for use of their ASHTECH GPS and processing software. The research was funded by the Commission of the European Community (DG XII), Environment Programme, Climatology and Natural Hazards Unit, through contract EV5V-CT92-0170; and by the Volcanic Hazards Advisory Committee of the Spanish Government. Finally, we would like to acknowledge the valuable contribution from Steve Saunders in the setting up of the ridge network and to thank Phil Gravestock and Steve Cooke for their assistance in the field.

References

Blewitt, G., 1997. Basics of the GPS technique: observation equations. In: Geodetic Applications of GPS. Swedish Land Survey.

Carracedo, J.C., 1994. The Canary islands: an example of structural control on the growth of large oceanic-island volcanoes. J. Volcanol. Geotherm. Res. 60, 225–241.

Carracedo, J.C., Day S.J., Guillou, H., 1997a. The Cumbre Nueva collapse and Cumbre Vieja volcano. In: International Workshop on Volcanism and Volcanic Hazards in Immature Intraplate Oceanic Islands, La Palma: Excursion Guidebook, pp. 1–28.

Carracedo, J.C., Day, S.J., Guillou, H., Badiola, E.R., Cana, J.A., Torrado, F.J.P., 1997b. Chronological, structural and morphological constraints on the genesis and evolution of the Canary Islands. Abstract. International Workshop on Volcanism and Volcanic Hazards in Immature Intraplate Oceanic Islands, La Palma.

Carracedo, J.C., Day, S.J., Guillou, H., Gravestock, P., 1997c. Geological colour map (1/33,000) of the Cumbre Vieja Volcano, La Palma, Canary Islands, 1st edn. Canary Islands: Consejo Superior de Investigaciones Cientificas and Cons. Politica Territorial, Gobierno Canarias.

Carracedo, J.C., Day, S.J., Guillou, H., Rodriguez Badiola, E., Canas, J.A., Perez Torrado, F.J., 1998. Hotspot volcanism close to a passive continental margin: the Canary Islands. Geol. Mag. 135, 591–604.

Carracedo, J.C., Day, S.J., Guillou, H., Gravestock, P. (in press). The later stages of the volcanic and structural evolution of La Palma, Canary Islands: the Cumbre Nueva giant collapse and the Cumbre Vieja Volcano. Geol. Soc. Am. Bull.

Crook, C.N., 1984. Geodetic measurements of horizontal crustal deformation associated with the October 15, 1979 Imperial Valley (California) earthquake. Thesis, Imperial College of Science and Technology, pp. 34–7623.

Day, S.J., Heleno da Silva, S.I.N., Fonseca, J.F.B.D., 1999. A past giant lateral collapse and present-day flank instability of Fogo, Cape Verde Islands. J. Volcanol. Geotherm. Res. 94, 191–210.

Delaney, P.T., Fiske, R.S., Miklius, A., Okamura, A.T., Sako, M.K., 1990. Deep magma body beneath the summit and rift-zones of Kilauea Volcano Hawaii. Science 247, 1265–1372.

Duffield, W.A., Stieltjes, L., Varet, J., 1982. Huge Landslide blocks in the growth of Piton de la Fournaise, La Reunion, and Kilauea Volcano, Hawaii. J. Volcanol. Geotherm. Res. 12, 147–160.

Dzurisin, D., Koyanagi, R.Y., English, T., 1984. Magma supply and storage at Kilauea Volcano, Hawaii. J. Volcanol. Geotherm. Res. 21, 177–206.

Elsworth, D., Voight, B., 1995. Dike intrusion as a trigger for large earthquakes and failure of volcano flanks. J. Geophys. Res. 100, 6005–6024.

Elsworth, D., Voight, B., 1996. Evaluation of volcano flank instability triggered by dyke intrusion. In: McGuire, W.J., Jones, A.P., Neuburg, J., (Eds.), Volcano Instability on the Earth and Other Planets. Geol. Soc. London, Spec. Publ. 110, pp. 45–53.

Funck, T., Schmincke, H.U., 1998. Growth and destruction of Gran Canaria deduced from seismic reflection and bathymetric data. J. Geophys. Res. 103, 15393–15407.

Guillou, H., Carracedo, J.C., Day, S.J., 1998. Dating of the Upper Pleistocene–Holocene volcanic activity of La Palma using the unspiked K–Ar technique. J. Volcanol. Geotherm. Res. 86, 137–149.

Hawaiian Volcano Observatory Monthly activity reports, 1966 to 1981. Hawaiian Volcano Observatory, Hawaii.

Hofmann-Wellenhof, B., Lichtenegger, H., Collins, J., 1997. Global Positioning System: Theory and Practice, 4th Ed. Springer-Verlag, Wien.

Holcomb, R.T., Searle, R.C., 1991. Large landslides from oceanic volcanoes. Mar. Geotechnol. 10, 19–32.

Masson, D., 1996. Catastrophic collapse of the volcanic island of El Hierro 15 ka ago and the history of landslides in the Canary Islands. Geology 24, 231–234.

McGuire, W.J., 1996. Volcano instability: a review of contemporary themes. In: McGuire, W.J., Jones, A.P., Neuberg, J. (Eds.), Volcano Instability on Earth and Other Planets. Geol. Soc. London, Spec. Publ., Vol. 110, pp. 1–24.

McGuire, W.J., Stewart, I.S., Saunders, S.J., 1997. Intra-volcanic rifting at Mount Etna in the context of regional tectonics. Acta Volcanol. 9 (1–2), 147–156.

Moss, J.L., 1999. The nature and operation of volcanic rift-zones, monitoring their role in the development of edifice instability and structural failure. PhD thesis, Cheltenham and Gloucester College of Higher Education, United Kingdom.

Murray, J.B., 1990. High-level magma transport at Mount Etna Volcano, as deduced from ground deformation measurements. In: Ryan, M.P. (Eds.), Magma Transport and Storage. Wiley, London, pp. 357–406.

Murray, J.B., Pullen, A., 1984. 3D model of the feeder conduit of the 1983 eruption of Mt. Etna volcano, from ground deformation measurements. Bull. Volcanol. 47/4 (2).

Nunnari, G., Puglisi, G., 1994. Ground deformation studies during the 1991–93 Etna eruption using GPS data. Acta Volcanol. 14, 101–107.

Nunnari, G., Puglisi, G., 1996. GPS — monitoring from space. In: McGuire, W.J., Kilburn, C.R.J., Murray, J.B. (Eds.), Monitoring Active Volcanoes. UCL Press, London.

Pollard, D.D., Delaney, P.T., Duffield, W.A., Endo, E.T., Okamura, A.T., 1993. Surface deformation in volcanic rift zones. Tectonophysics 94, 541–584.

Savage, J.C., Prescott, W.H., 1997. Precision of geodolite distance measurements for determining fault movements. J. Geophys. Res. 78, 26.

Swanson, D.A., Duffield, W.S., Fiske, R.S., 1976. Displacement of the south flank of Kilauea Volcano: the result of forceful intrusion of magma into the Rift Zones. US Geol. Surv. Prof. Pap., p. 963.

Uren, J., Price, W.F., 1994. Surveying for Engineers, 3rd edn. Macmillan, London.

Walker, G.P.L., 1990. Geology and volcanology of the Hawaiian islands. Pacific Sci. 44, 315–347.

Yang, X., Davis, P., Delaney, P., Okamura, A., 1992. Geodetic analysis of dike intrusion and motion of the magma reservoir beneath the summit of Kilauea Volcano, Hawaii: 1970–1985. J. Geophys. Res. 97 (B3), 3305–3324.